Induced Coalescence of Cations through Low-Temperature Poisson-Boltzmann Calculations

Gene Lamm and George R. Pack
Department of Chemistry, University of Louisville, Louisville, Kentucky 40292

ABSTRACT The computational determination of preferred binding regions of divalent counterions to nucleic acids is either inaccurate (standard Poisson-Boltzmann approaches) or extremely time-consuming (Monte Carlo or molecular dynamics simulations). A novel "selective low-temperature" Poisson-Boltzmann method is introduced that, although approximate in nature, qualitatively accounts for ion correlation and charge-transfer effects and allows for the rapid determination of such regions through an "induced coalescence" of divalent ions. The method is illustrated here for the binding of Mg^{2+} to a double-helical sequence of B-form DNA (CGCGAATTCGCG) but the technique is readily applicable to locating divalent cations in other systems such as DNA-endonuclease complexes and ribozymes.

INTRODUCTION

The binding of cations to nucleic acids has been the focus of a variety of experimental and theoretical methods (Anderson and Record Jr., 1995). Whereas monovalent counterions interact with nucleic acids mainly through a mobile association dominated by electrostatic attraction, (Anderson and Record Jr., 1990), the interaction of divalent counterions is strongly influenced by the presence of a stable hydration shell. Outersphere coordination of divalent cations to proton acceptors gives rise to localized binding in specific regions at the macromolecular surface. We present here a simple computational method to predict these divalent counterion binding domains where standard approaches fail.

Magnesium is unusual among divalent cations in that its hydration shell is smaller and more tightly bound than most, which may account for its presence as a cofactor in a number of biochemical reactions. This layer of bound water molecules not only shields the cation-DNA electrostatic attraction and increases the distance of closest approach between the cation and DNA, it also allows for the formation of hydrogen bonds with specific base atoms (Petrov et al., 2002,2004). Spectroscopic studies suggest that water molecules bind tighter to divalent cation-DNA complexes than to DNA alone (Andrushchenko et al., 1997), which by itself could increase water-mediated protein-DNA specificity. Magnesium is the preferred cation in most site-specific hydrolysis reactions involving type II restriction endonucleases, such as *Eco*RI and *Eco*RV (Jeltsch et al., 1993; Vipond et al., 1995). Magnesium is also intimately involved in the formation of RNA tertiary structure (Tinoco Jr. and Bustamante, 1999) where it binds to a variety of different regions such as in the major or minor groove or to the phosphate backbone (Chiu and Dickerson, 2000; Robinson et al., 2000; Adamiak et al., 2001; Juneau et al., 2001; Ennifar et al., 2001; Zhang and Doudna, 2002). A clear vision of the mechanism of Mg^{2+}-nucleic acid interactions would thus impact our understanding of many biochemical reactions and a first step toward this is the elucidation of preferential magnesium binding regions.

Whereas general counterion association around nucleic acids is primarily electrostatic in nature and is adequately described on the basis of either Manning's theory (Manning, 1978) or the Poisson-Boltzmann (PB) equation (Anderson and Record Jr., 1990; Lamm, 2003), neither approach is easily adapted to site-specific interactions between the first hydration shell of magnesium and proton acceptors on the nucleic acid surface. Also, the traditional PB approach, although numerically efficient and readily applicable to large systems, produces counterion distributions that are too broad, particularly for divalent ions (Anderson and Record Jr., 1990; Pack et al., 1999). This is in part due to neglect of nonelectrostatic contributions to the free energy, such as correlation effects and van der Waals, and hydrogen bonding. An improved treatment would require use of all-atom Monte Carlo or molecular dynamics simulations. However, these methods are computationally time-consuming and tend to sample limited regions of the free energy surface, especially for large macromolecules where ions can become trapped in local potential wells. Unfortunately it is these potential wells that are also inadequately represented by the PB equation.

An approximate way out of this conundrum is to realize that most of the nonelectrostatic free energy contributions that deepen regions of the potential surface of divalent cation-nucleic acid interactions occur at the solvent interface in roughly the same region where electrostatic attraction is largest. The electrostatic potential obtained by coupling the Poisson equation for fixed (macromolecular) and mobile (ionic) charges (Anderson and Record Jr., 1990; Lamm, 2003),

Submitted January 15, 2004, and accepted for publication April 12, 2004.

Address reprint requests to George R. Pack, Professor and Chair, Dept. of Chemistry, University of Louisville, 2320 South Brook St., Louisville, KY 40292. Tel.: 502-852-6798; E-mail: george.pack@louisville.edu.

0006-3495/04/08/764/04 $2.00

doi: 10.1529/biophysj.104.040220

$$\nabla \cdot \varepsilon(\underline{r}) \cdot \nabla\psi(\underline{r}) = -4\pi(\rho^{\text{fixed}}(\underline{r}) + \rho^{\text{mobile}}(\underline{r})), \quad (1)$$

to the (mean-field) Boltzmann equation,

$$\rho^{\text{mobile}}(\underline{r}) = \sum_{\text{i}} e_0 z_{\text{i}} c_{\text{i}} e^{-\beta e_0 z_{\text{i}} \psi(\underline{r})}, \quad (2)$$

satisfies a balance between electrostatic and entropic components (Eqs. 1 and 2, respectively). The source of error in the PB solution for hydrated divalent cation binding relative to that for monovalent ions might be interpreted as an increase in the entropic component at the expense of the electrostatic one. Thus, by moving some of the entropic free energy to the electrostatic side of the balance sheet, the distribution of divalent cations could be improved. (In Eqs. 1 and 2, $\varepsilon(\underline{r})$ is the value of the local dielectric coefficient, $\beta = 1/k_{\text{B}}T$ defines the system temperature, e_0 is the proton charge, z_{i} denotes the valence of ionic species i, c_{i} denotes the concentration of species i at some reference point in the system which also defines the gauge of the potential—typically $\psi = 0$ either at an outer boundary or at infinity.) This view is supported by the numerous crystal structure determinations in which magnesium ions and their concomitant hydration shell are located but in which sodium ions are not. If, on the basis of the above balancing argument, one reinterprets this as a difference in their *B*-factors, then one might view magnesium ions as being ''cooler'' than the sodium ions. One might equally argue that magnesium binding is different from sodium binding in that the former involves nonelectrostatic components, such as charge transfer and polarization, that are not accounted for in a purely electrostatic standard PB approach, a point to which we will return at the end of this article. As seen from Eq. 2, decreasing the temperature of magnesium ions is equivalent to increasing the mean potential $e_0 z\psi$. Thus, either interpretation may be readily incorporated into the PB method by introducing a lower temperature for the magnesium ion species in Eq. 2 than that used for sodium. To illustrate the effect of doing so, we now present a specific example.

RESULTS AND DISCUSSION

We considered a length of double stranded B-form DNA (CGCGAATTCGCG) extended along the *z*-direction and immersed in an electrolyte bath containing 100 mM NaCl and 20 mM $MgCl_2$ at 298 K. A rolling-sphere algorithm was used to lay down points in a series of *x*-*y* planes with points in each plane distributed in layers, with each layer more distant from the macromolecular surface than the previous, extending out to a radius of 177 Å (corresponding to a phosphate concentration of 10 mM); the interior of the macromolecule was also gridded (Klein and Pack, 1983; Pack et al., 1999). This method generates a space-filling set of Voronoi polyhedra whose elements are assigned spatial positions, volumes and initial dielectric coefficients and the overlapping surface areas with neighboring elements tabulated. (The PB modification described below does not require any particular method of point assignment—the more common cubic gridding procedure works equally well—but the method used here permits some additional observations to be made.) Inner-layer widths of 1.1 Å, 0.8 Å, and 0.8 Å were chosen to restrict sodium ions (considered as 1.1 Å radius spheres) to layers 2 and greater, to restrict hexahydrated magnesium ions (considered as 2.7 Å radius spheres) to layers 4 and greater, and to provide adequate discretization of space. Also, chloride anions were treated as 2.7 Å spheres, interior DNA grid points were placed 1.0 Å apart and vertical planes were separated by 1.13 Å. These space-filling polyhedra are used in the initial value assignments, in defining ion exclusion layers, and in the numerical solution of the PB equation and its subsequent analysis (Pack et al., 1999). A 15-basepair segment was chosen and replicated once above and once below the central segment to reduce end effects. The finite-difference representation of Eqs. 1 and 2 was then iterated until convergence. The spatially-dependent dielectric coefficients $\varepsilon(\underline{r})$ were calculated self-consistently using previously derived expressions that take into account high electric fields due to DNA surface charges and/or high local ion concentrations (Pack et al., 1993; Lamm and Pack, 1997). (Variable dielectric coefficients are also unnecessary to the PB modification at hand but are a welcome inclusion as will be noted below.)

Fig. 1 displays converged sodium (*above*) and magnesium (*below*) concentrations as contour plots in the plane of a C-G basepair; the major groove is oriented toward the lower left corner of each plot. Concentration contours are shown every 2 M for the range 0–20 M and all plots are drawn to the same scale. The left-most column displays data from the standard PB calculation in which the system temperature is 298 K, showing high sodium concentrations in the accessible minor groove at the top and somewhat lower values in the major groove. Magnesium concentrations are lower with maximum values lying in the major groove, as evidenced by the very small contour; the much larger distance of closest approach to the surface is obvious when compared with the sodium plot above it. Although some agreement with a known preference of magnesium for guanine O6 and N7 atoms is suggested by the lone major groove contour, one could hardly use this as evidence that the PB approach is useful in identifying this as a specific binding region (Chiu and Dickerson, 2000; Robinson et al., 2000; Adamiak et al., 2001; Ennifar et al., 2001; Juneau et al., 2001). Furthermore, the paucity of structure (even upon viewing the numerical data) offers little help in determining other divalent binding regions such as anionic phosphate oxygens (Robinson et al., 2000; Adamiak et al., 2001; Ennifar et al., 2001; Juneau et al., 2001; Zhang and Doudna, 2002).

Reading Fig. 1 from left to right illustrates the effect of selectively lowering the magnesium temperature from 298 K

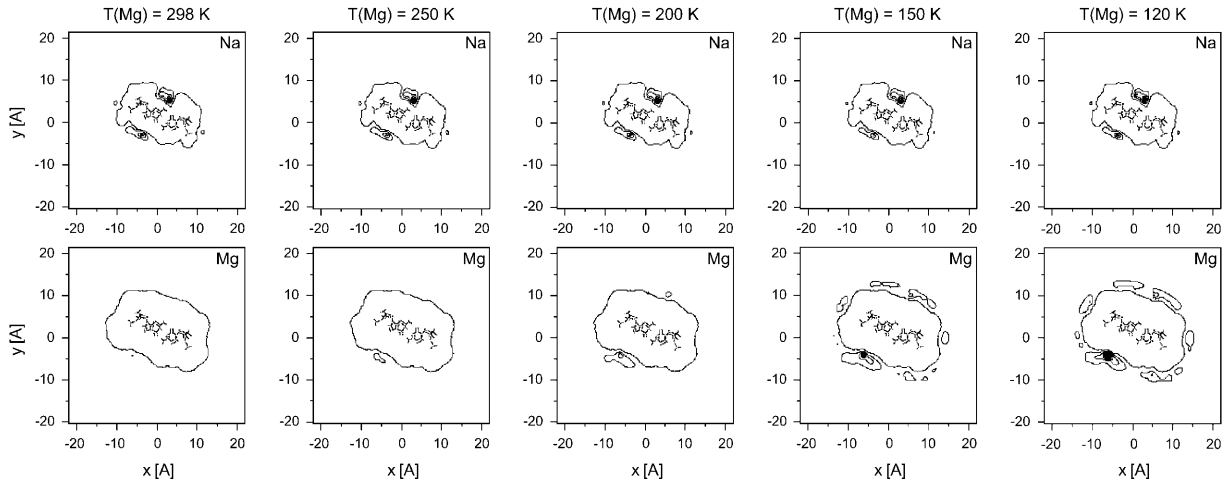

FIGURE 1 Contour plots of PB-calculated sodium and magnesium counterion concentrations in a cross-sectional plane surrounding a C-G basepair of double-helical B-form DNA; the major groove lies across the lower left side of the small all-atom inset. Contours are plotted every 2 M from 0 to 20 M with sodium concentrations shown in the top row and magnesium concentrations in the bottom. The sodium temperature (see text) was fixed at 298 K with the magnesium temperature varying from 298 K (*left-most column*) to 120 K (*right-most column*). Electrolyte conditions were 100 mM monovalent salt (NaCl) and 20 mM divalent salt ($MgCl_2$) with sodium ions modeled as 1.1 Å spheres and magnesium and chloride ions as 2.7 Å spheres.

to 250 K, 200 K, 150 K, and 120 K. Little change is seen in the sodium distribution as a function of the magnesium temperature; the sodium temperature was kept at 298 K but the sodium distribution is still coupled to the magnesium distribution through the Eq. 2. As the magnesium temperature is lowered, primary and secondary patterns of ''induced coalescence'' begin to emerge. At $T(Mg) = 120$ K, the main binding site near the O6 and N7 atoms of guanine is prominent but secondary sites near the phosphate groups begin to appear. Note also that the binding pattern just outside the minor groove is separated into two regions by the strong competitive influence of sodium ions within the groove.

An alternative to the low-temperature PB procedure suggested here would be simply to artificially increase the valence on the magnesium ion in order give more weight to the electrostatic contribution to the free energy. Within the Debye-Hückel approximation the two procedures (low-temperature versus increased valence) are equivalent. However, the Debye-Hückel approximation is known to be particularly poor both for multivalent ions and for highly charged polyelectrolytes; for magnesium ions at 150 K, the resulting valence (at 298 K) is ~3. (It is easily shown that decreasing the temperature of an ion in the PB equation is equivalent to increasing the ion's valence while decreasing its concentration.) If a standard PB calculation is performed under the same conditions as Fig. 1 but with a valence of $z = 3$ for the multivalent cation, one finds much lower surface concentrations, and hence much less regional specificity, of ''M^{3+}'' (at $T = 298$ K) compared to Mg^{2+} (at $T = 150$ K).

A comment concerning the inclusion of local dielectric coefficients needs to be made. As divalent ion coalescence occurs in different spatial regions throughout the system, the dielectric coefficient in those regions drops, approaching that representative of the pure ion (a value of 2 was used here). Because the PB equation was solved self-consistently including local dielectric changes, the energy-lowering that results from two (or more) low dielectric cavities being clustered together (mutual ''solvation'') is automatically taken into account.

Finally, we remark that although the reduced-temperature divalent counterion patterns demonstrate the desired behavior, the underlying numerical data are only of semiquantitative significance. One could make partial occupancy assignments based on the total counterion charge within a specific region of space, but a more detailed analysis would require some energy-based justification for assigning a particular reduced temperature. Lowering the temperature of a selected ionic species is an attempt to account for neglected aspects of PB theory such as ion correlation, van der Waals interactions or hydrogen bonding. As long as these components operate in approximately the same spatial region as the electrostatic component, the results should be informative. A first step in ''calibrating'' the temperatures of both ionic species (sodium as well as magnesium) could be to obtain reasonable fits to Monte Carlo data for charged cylinders. This would provide some compensation for the often-noted lack of ion correlation and ion size within PB theory as well as offer a simpler computational alternative to modified PB theories (Lamm, 2003). One might extend this calibration by comparing low-temperature PB binding sites with those observed in small-molecule DNA and RNA crystal structures and in so doing obtain an estimate of the average magnesium binding energy in these systems. However, many of these binding sites span two nucleic acid molecules. To account for those cases, it might be necessary to solve the PB equation subject to boundary conditions at the surface of the appropriate unit cell. Recent calculations of

the total binding energy for magnesium-guanine and magnesium-dimethylphosphate using B3LYP/6-31G(d,p) with CPCM give energies (in water) to be ~ -20 kcal/mol and -30 kcal/mol, respectively, for the optimized complexes, almost all of which is nonelectrostatic in origin (i.e., charge transfer, polarization, and exchange) (Petrov et al., 2004). How much of this nonclassical binding energy contributes to the potential of mean force in magnesium-nucleic acid interactions is difficult to determine (one would need to average the interactions spatially and in the presence of added salt), but this clearly points out that significant energy contributions are neglected in standard PB calculations. The low-temperature modification appears to be a computationally simple means of improving upon a much-used approach.

In this article we have restricted our treatment to a molecule with approximate axial symmetry to more clearly demonstrate the results, but nothing in the development prevents the application of low-temperature PB to less symmetric systems such as DNA-endonuclease complexes or RNA molecules. We also note that the low-temperature PB method should also be useful in suggesting more efficient starting configurations for all-atom Monte Carlo or molecular dynamics simulations involving multivalent ions and highly charged macromolecules.

REFERENCES

Adamiak, D. A., W. R. Rypniewski, J. Milecki, and R. W. Adamiak. 2001. The 1.19 angstrom X-ray structure of 2 '-O-Me(CGCGCG)(2) duplex shows dehydrated RNA with 2-methyl-2,4-pentanediol in the minor groove. *Nucleic Acids Res.* 20:4144–4153.

Anderson, C. F., and M. T. Record Jr. 1990. Ion distributions around DNA and other cylindrical polyions – theoretical descriptions and physical implications. *Annu. Rev. Biophys. Biophys. Chem.* 19:423–465.

Anderson, C. F., and M. T. Record Jr. 1995. Salt nucleic-acid interactions. *Annu. Rev. Phys. Chem.* 46:657–700.

Andrushchenko, V. V., S. V. Kornilova, L. E. Kapinos, E. V. Hackl, V. L. Galkin, D. N. Grigoriev, and Y. P. Blagoi. 1997. IR-spectroscopic studies of divalent metal ion effects on DNA hydration. *J. Mol. Struct.* 408:225–228.

Chiu, T. K., and R. E. Dickerson. 2000. 1 angstrom crystal structures of B-DNA reveal sequence-specific binding and groove-specific bending of DNA by magnesium and calcium. *J. Mol. Biol.* 301:915–945.

Ennifar, E., P. Walter, B. Ehresmann, C. Ehresmann, and P. Dumas. 2001. Crystal structures of coaxially stacked kissing complexes of the HIV-1 RNA dimerization initiation site. *Nat. Struct. Biol.* 8:1064–1068.

Jeltsch, A., J. Alves, H. Wolfes, G. Maass, and A. Pingoud. 1993. Substrate-assisted catalysis in the cleavage of DNA by the EcoRI and EcoRV restriction enzymes. *Proc. Natl. Acad. Sci. USA.* 90:8499–8503.

Juneau, K., E. Podell, D. J. Harrington, and T. R. Cech. 2001. Structural basis of the enhanced stability of a mutant ribozyme domain and a detailed view of RNA-solvent interactions. *Structure.* 9:221–231.

Klein, B. J., and G. R. Pack. 1983. Calculations of the spatial-distribution of charge-density in the environment of DNA. *Biopolymers.* 22:2331–2352.

Lamm, G. 2003. The Poisson-Boltzmann equation. *Rev. Comput. Chem.* 19:147–365.

Lamm, G., and G. R. Pack. 1997. Calculation of dielectric constants near polyelectrolytes in solution. *J. Phys. Chem. B.* 101:959–965.

Manning, G. S. 1978. Molecular theory of polyelectrolyte solution with application to electrostatic properties of polynucleotides. *Quart. Rev. Biophys.* 11:179–246.

Pack, G. R., G. A. Garrett, L. Wong, and G. Lamm. 1993. The effect of a variable dielectric coefficient and finite ion size on Poisson-Boltzmann calculations of DNA-electrolyte systems. *Biophys. J.* 65:1363–1370.

Pack, G. R., L. Wong, and G. Lamm. 1999. Divalent cations and the electrostatic potential around DNA: Monte Carlo and Poisson-Boltzmann calculations. *Biopolymers.* 49:575–590.

Petrov, A. S., G. Lamm, and G. R. Pack. 2002. Water-mediated magnesium-guanine interactions. *J. Phys. Chem. B.* 106:3294–3300.

Petrov, A. S., G. R. Pack, and G. Lamm. 2004. Calculations of magnesium-nucleic acid site binding in solution. *J. Phys. Chem. B.* 108:6072–6081.

Robinson, H., Y.-G. Gao, R. Sanishvii, A. Joachimiak, and A. H. J. Wang. 2000. Hexahydrated magnesium ions bind in the deep major groove and at the outer mouth of A-form nucleic acid duplexes. *Nucleic Acids Res.* 28:1760–1766.

Tinoco, I. Jr., and C. Bustamante. 1999. How RNA folds. *J. Mol. Biol.* 293:271–281.

Vipond, I. B., G. S. Baldwin, and S. E. Halford. 1995. Divalent metal-ions at the active-sites of the EcoRV and EcoRI restriction endonucleases. *Biochemistry.* 34:697–704.

Zhang, L., and J. A. Doudna. 2002. Structural insights into group II intron catalysis and branch-site selection. *Science.* 295:2084–2088.